Mechanic and Energy
Mecânica e Energia

Application of optimization for improvement of the efficiency of louvered-fin compact heat exchangers

http://dx.doi.org/10.1590/0370-44672016690003

Diego Amorim Caetano Souza
Mestrando
Universidade Federal de São João Del Rei - UFSJ
Programa de Pós graduação Engenharia da Energia - PPGEE
São João Del Rei – Minas Gerais - Brasil
diegomec8@gmail.com

Luben Cabezas Gómez
Professor Doutor
Universidade de São Paulo - USP
Departamento de Engenharia Mecânica
Escola de Engenharia de São Carlos - EESC
São Carlos – São Paulo – Brasil
cab35ezas@yahoo.com.br

José Antônio Silva
Professor Associado
Universidade Federal de São João Del Rei - UFSJ
Programa de Pós Graduação em Engenharia de Energia
Departamento de Ciências Térmicas e dos Fluídos
São João Del Rei – Minas Gerais - Brasil
jant@ufsj.edu.br

Julio Cesar Costa Campos
Professor Adjunto
Universidade Federal de Viçosa - UFV
Departamento de Engenharia de Produção e Mecânica
Viçosa – Minas Gerais - Brasil
juliomcampos20@gmail.com

Abstract

A few decades ago, the product development process was just based on a trial and error procedure, and the designer's experience. The need for a new way to design and manufacture more economical and sustainable products corroborates increasingly to a new vision of how to create new products for the benefit of society. Modern numerical tools allow greater knowledge about the physical phenomena involved in engineering problems and enable cost reduction with trials and time of manufacture and projection.

Among the equipment that can be mentioned where numerical simulation is used, can be found heat exchangers, which are capable of accomplishing the heat transfer between two fluid medias with different temperatures. Within the range of existing exchangers, this work will address a compact model with louvered fins, widely used in the automotive and aerospace industries, mainly due to their high thermal exchange surface vs occupied volume ratio. The heat exchanger surface is analised using computational fluid dynamics tecniques disposable in the commercial code ANSYS CFX14® to reproduce the flow at service condition. Genetic optimization routines are used to increase the performance of heat exchanger. As a result, a heat transfer surface is obtained with about a 25% better performance according to the selected objective function. The dimensionless factor of the convective heat transfer coefficient (Colburn factor, j) and the friction factor (Fanning factor, f) used in (Wang *et al.*,1998), are employed for simulation. Experimental data are also used for validation.

keywords: compact heat exchanger, CFD, optimization, louver fins.

1. Introduction

The design of more efficient thermal equipment with lower cost is one of the goals of modern engineering. Processes and very sophisticated tools are used to increasingly achieve optimized and competitive components.

Thus, the use of numerical simulation and optimization algorithms become tools to achieve results, change the initial prototypes by virtual tests, reducing costs associated with the reduction of experimental trials (Herckert *et al.*, 2004). The numerical analyses also allow better understanding of the phenomena involved.

In the present work a compact heat exchanger with louvered fins is analyzed by reproducing the flow at service condition using computational tools. These fins are fabricated by the stamping of sheet metal and the bending of the cut region, allowing a massflow between layers and increasing the heat transfer rate due to their influence on the flow and temperature behavior. Due to the effects caused by the louvered fins, it is necessary to perform CFD simulations as well as to apply optimization procedures to find the best arrangements of louvered fin angles.

Compact heat exchangers are frequently used in automotive and aerospace industries due to their compactness represented by a relationship between the heat transfer area and a volume higher than 700 m^2/m^3. The presented procedure is valid for incompressible flows and is restricted to the applied boundary conditions and geometrical restriction. However the procedure can be used in more refined studies considering other flow conditions and a full heat exchanger surface.

Nomenclature

C_P - Specific Heat
D_C - Internal diameter
$F_1, F_2, F_3, F_4, F_5, F_6, F_7, F_8, F_9$ – Correlation parameters for the Fanning factor
f_{high} - Fanning factor for a high Reynolds number
f_{low} - Fanning factor for a low Reynolds number
F_d- Fin depth
F_p- Fin Pitch
G– Objective function
$J_1, J_2, J_3, J_4, J_5, J_6, J_7, J_8$ - Correlation parameters for the Colburn factor
j_{high} - Colburn factor for a high Reynolds number
j_{low} - Colburn factor for a low Reynolds number
K- Turbulent kinetic energy
L– Characteristic length
L_h- Louver height
L_p- Lover pitch
N- Quantity of tubes
P, p- Pressure
P_l- Longitudinal tube Pitch
P_t- Transverse tube Pitch
T, t- Temperature
u- Longitudinal Velocity
U_{max}- Maximum velocity in vertical section with smaller area
u^* - Fluid friction velocity near the wall
x -Variable in x direction
y - Distance to the wall
y^+ - Dimensionless distance to the wall

Greek Symbols

ε - Dissipation rate of turbulent kinetic energy
μ - Dynamics viscosity
υ - Kinematic viscosity
ρ- Density
ω- Specific dissipation of turbulent kinetic energy

2. Materials and methods

The ANSYS CFX® commercial software is used to perform the fluid dynamic analysis with the finite volume method (FVM), based on the solution of equations of mass, energy and momentum conservation (Maliska, 2004), exhibited by equations 1, 2 and 3 respectively.

$$\frac{\partial \rho}{\partial t} + \frac{\partial}{\partial x_j}\left(\rho u_j\right) = 0 \tag{1}$$

$$\frac{\partial}{\partial t}\left(\rho u_i\right) + \frac{\partial}{\partial x_j}\left(\rho u_j u_i\right) = -\frac{\partial P}{\partial x_i} + \frac{\partial}{\partial x_j}\left(\mu \frac{\partial u_i}{\partial x_j}\right) + S^{u_i} \tag{2}$$

$$\frac{\partial}{\partial t}\left(\rho T\right) + \frac{\partial}{\partial x_j}\left(\rho u_j T\right) = \frac{\partial}{\partial x_j}\left(\frac{k}{c_p}\frac{\partial T}{\partial x_j}\right) + S^T \tag{3}$$

After the development of the computational procedure, the flow and temperature field variables are analyzed and the required dimensionless variables of interest (friction, *f*, and Colburn, *j*, factors) are also computed.

For turbulence modeling, the SST (Shear Stress Transport) turbulence model is used, which belongs to the family of RANS (Reynolds Averaged Navier-Stokes).

Developed by (Menter, 1994), this model was largely applied to calculate aerodynamic complex flows with adversely pressure gradients, as generally detected in airfoils.

Traditional models fail to capture these phenomena due to the degree of complexity and nonlinearity. To overcome these difficulties, the SST model (Menter, 1994), used two models, the *k* - ε and *k* – ω.

The *k* - ω is applied to estimate the fluid characterization in regions near the wall where the flows are more complex, and the *k* - ε model is applied in regions far from the walls, where the turbulence phenomena are weaker and the shear stresses are lower, mainly because the ω property is sensible for these regions, reducing the precision of the model.

So, as the distance decreases in relation to the wall ε calculation, it is replaced by ω computation. The blending function is applied to command the alteration of these variables.

To use the SST model properly, it is necessary to adopt some quality criteria. Among them, the dimensionless distance parameter to the wall, y^+, calculated by the following expression, must remain less than 1 in the mesh nodes near the wall for proper operation of the SST model. In equation 4, *y* is the distance from the wall, u^* is the fluid friction velocity near the wall, υ is the kinematic viscosity of the fluid and y^+ is the dimensionless distance.

$$y^+ = \frac{u^* y}{\upsilon} \tag{4}$$

In this work, a heat exchanger with fins of louver type is simulated. This model has repeated oblique cuttings created on the main sheet in the manufacturing process.

This operation enables the passing of the working fluid of heat exchanger between sheets. Due to this, the fluid molecules remain more time in the domain, remove more increase its thermal energy and enhance the heat transfer.

Turbulence is a phenomenon of dissipative nature and helps to increase the energy exchange. In the simulated type of heat exchanger, the heat exchange is enlarged due to the louvered fins that can be designed to be vortex generators. The mixture region formed by turbulence favors the energy transport of warm fluid which flows through the tubes to the cold external

fluid. The behavior of the fluid flowing through the external cold side is one of the objects of the study performed in this work.

Compact heat exchangers are generally formed by a repeating geometric pattern. For this reason, the studied volume can be divided into reduced cells, and the analysis can be performed for a single cell device (Michael, 2006). This allows reduction of the computational effort and time spent waiting for the results. Consequently, optimization processes such as those utilized in this work that perform various simulations in series become feasible.

Used in this work are data obtained by (Wang *et al.*,1998), through physical analysis in specific equipment, and the numerical simulations performed by (Jang and Chen, 2013), in commercial code as presented herein.

For domain creation, sections are inserted before the inlet of cell (one time the internal diameter) and after the end (seven times the internal diameter) to prevent abrupt behavior variations, as recommended by (Perrotin and Clodic, 2004), to facilitate the convergence.

The main dimensions utilized for heat exchanger domain are shown in Figure 1 and its values are presented in Table 1.

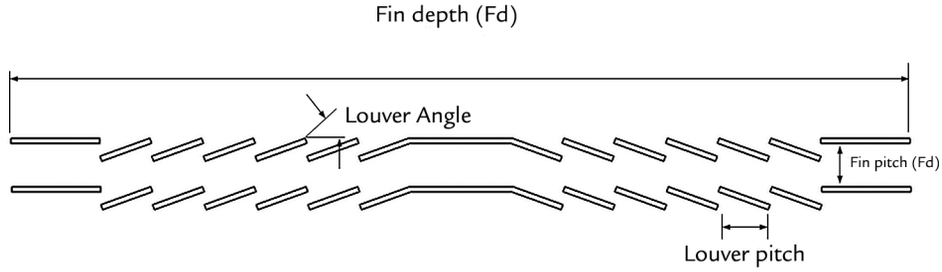

Figure 1
Main dimensions of heat exchanger.

Main Dimensions	Fin depth (F_d)	Fin pitch (F_p)	Louver pitch (L_p)	External tube diameter	Quantity of tubes (N)	Fins thickness	Louver angle
Default Value (degrees or mm)	38.00	2.050	2.40	10.42	2.00	0.115	25.00

Table 1
Geometrical dimensions of the fin used.

The element type utilized is the tetrahedral element, recommended for its adaptability to complex geometries. To reach a value of y^+ near 1, the edges of elements are computerized as 0.5 millimeter, resulting in a mesh around 1.97E+5 elements and 6E+4 nodes. Details of mesh are illustrated in Figures 2 and 3.

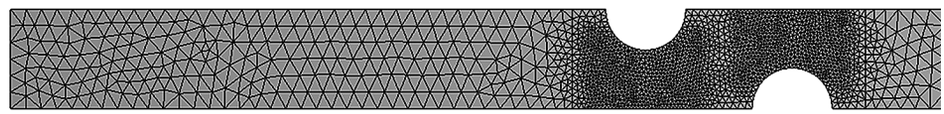

Figure 2
Mesh of domain.

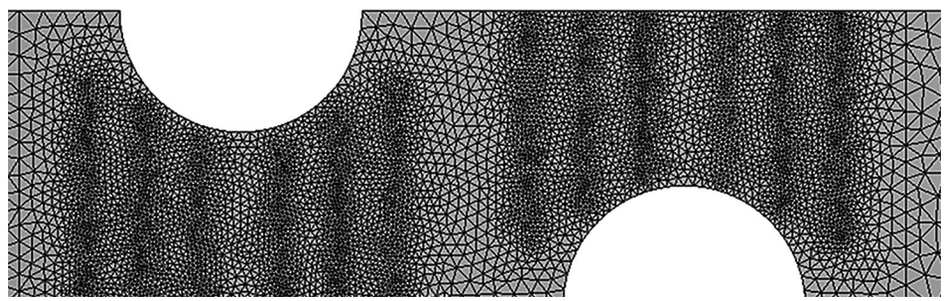

Figure 3
Mesh details in the fins.

The Reynolds number is calculated by equation 5 and it is used as an output variable, to compute the dimensionless numbers *f* and *j*.

In the entrance domain, the air flows from 0.50 to 7.50m/s with 300,0K. The tubes have a wall temperature of 353. 0K

$$Re = \frac{\rho U_{máx} L}{\mu} \quad (5)$$

- U_{max}: means the maximum velocity in vertical section with smaller area – the flow is considered incompressible due to the low velocity values.
- L: is the characteristic length

The boundary conditions are displayed in Figures 4 and 5. At the wall surfaces of tubes and fins, the no slip boundary condition is applied. This condition assumes that the fluid velocity at the wall equals to zero. Symmetry is assumed in the lateral faces of the domain and in the upper and bottom faces of the domain, a periodic condition is used.

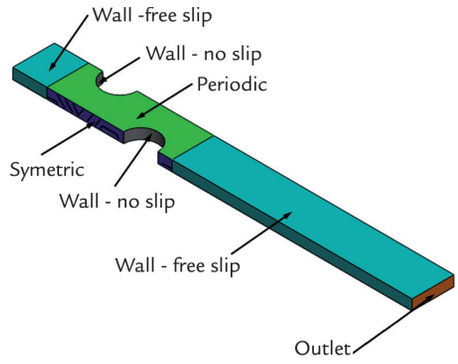

Figure 4
Domain and applied boundary conditions.

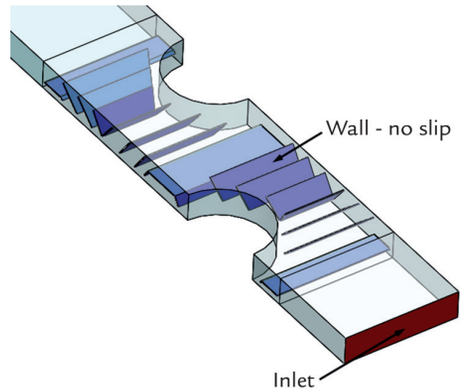

Figure 5
Boundary conditions used in the fins.

In the post-processing phase, after solving the systems of equations, the output variable generated is the Reynolds number, obtained by equation 2 and the friction and Colburn factors *f* and *j*, obtained by a procedure developed by (Wang *et al.*,1998). These authors experimentally analyzed 49 louvered-fin heat exchangers and developed the f and j correlations used in this work. The reference (Weber, 2007), found similar correlations for Colburn and fanning factors by physical tests.

For a low Reynolds number (lower than 1000), the j_{low} is calculated by equation 6 using the exponents of equations 7, 8, 9 and 10 (J_1, J_2, J_3 and J_4).

$$j_{low} = 14{,}3117\, Re_{Dc}^{J_1} \left(\frac{F_p}{D_c}\right)^{J_2} \left(\frac{F_h}{L_p}\right)^{J_3} \left(\frac{F_p}{P_l}\right)^{J_4} \left(\frac{P_l}{P_t}\right)^{-1{,}724} \tag{6}$$

$$j_1 = -0{,}991 - 0{,}1055 \left(ln\left(\frac{L_h}{L_p}\right)\right) \left(\frac{P_l}{P_t}\right)^{3{,}1} \tag{7}$$

$$j_2 = -0{,}7344 + 2{,}1059 \left(\frac{L_h}{ln\,(Re_{Dc}) - 3{,}2}\right) \tag{8}$$

$$j_3 = 0{,}08485 \left(\frac{P_l}{P_t}\right)^{-4{,}4} N^{-0{,}68} \tag{9}$$

$$j_4 = -0{,}1741\, ln\,(N) \tag{10}$$

For high Reynolds number (higher than 1000), the j_{high} is calculated by equation 11 using the exponents of equations 12, 13, 14 and 15 (J_9, J_{10}, J_{11} and J_{12}).

$$j_{high} = 1{,}1373\, (Re_{Dc}^{J_5}) \left(\frac{P_p}{P_l}\right)^{J_6} \left(\frac{L_h}{L_p}\right)^{J_7} \left(\frac{P_l}{P_t}\right)^{J_8} N^{0{,}3545} \tag{11}$$

$$j_5 = -0{,}6027 + 0{,}02593 \left(\frac{P_l}{D_h}\right)^{0{,}52} \left(ln\left(\frac{L_h}{L_p}\right)\right) N^{-0{,}5} \tag{12}$$

$$j_6 = -0{,}4776 + 0{,}40774 \left(\frac{N^{0{,}7}}{ln\,(Re_{Dc}) - 4{,}4}\right) \tag{13}$$

(14) $$j_7 = -0{,}58655\left(\frac{F_p}{D_h}\right)^{2,3}\left(\frac{P_l}{P_t}\right)N^{-0,65}$$

(15) $$j_8 = 0{,}0814\,(ln\,(Re_{Dc})\,-3\,)$$

In the same way, the *f* factor is calculated for the low and high Reynolds number. For *Re* lower 1000, f_{low} is calculated by equation 16 with exponents F_1, F_2, F_3 and F_4 extracted from equations 17 to 20.

(16) $$f_{low} = 0{,}00317\,(Re_{Dc})\,\left(\frac{F_p}{P_l}\right)^{F_2}\left(\frac{D_h}{D_c}\right)^{F_3}\left(\frac{L_h}{L_p}\right)^{F_4}\left(ln\left(\frac{A_0}{A_t}\right)\right)^{-6,0483}$$

(17) $$F_1 = 0{,}1692 + 4{,}4118\left(\frac{F_p}{P_l}\right)^{-0,3}\left(\frac{L_h}{L_p}\right)^{-2}\left(ln\left(\frac{P_l}{P_t}\right)\right)\left(\frac{F_p}{P_t}\right)^{3}$$

(18) $$F_2 = -2{,}6642 - 14{,}3809\left(\frac{1}{ln\,(Re_{Dc})}\right)$$

(19) $$F_3 = -0{,}6816\left(ln\left(\frac{F_p}{P_l}\right)\right)$$

(20) $$F_4 = 6{,}4668\left(\frac{F_p}{P_t}\right)^{1,7}\left(ln\left(\frac{A_0}{A_t}\right)\right)$$

f_{high} is found by equation 21 with exponents (F_{19}, F_{20}, F_{21}, F_{22} and F_{23}) of equation 22 to 26.

(21) $$f_{high} = 0{,}06393\,(Re_{Dc}^{F_5})\left(\frac{F_p}{D_c}\right)^{F_6}\left(\frac{D_h}{D_c}\right)^{F_7}\left(\frac{L_h}{L_p}\right)^{F_8}N^{F_9}\,(ln\,(Re_{Dc})\,-4)^{-1,093}$$

(22) $$F_5 = 0{,}1395 - 0{,}0101\left(\frac{F_p}{P_l}\right)^{0,58}\left(\frac{L_h}{L_p}\right)^{-2}\left(ln\left(\frac{A_0}{A_t}\right)\right)\left(\frac{P_l}{P_t}\right)^{1,9}$$

(23) $$F_6 = -6{,}4367\left(\frac{1}{ln\,(Re_{Dc})}\right)$$

(24) $$F_7 = 0{,}05875\,(ln\,(Re_{Dc}))$$

(25) $$F_8 = -2{,}0585\left(\frac{F_p}{P_t}\right)^{1,67}(ln\,(Re_{Dc}))$$

(26) $$F_9 = 0{,}1036\left(ln\left(\frac{P_l}{P_t}\right)\right)$$

The values of the output variables *f* and *j* are compared with the experimental data obtained in (Wang *et al.*,1998). After obtaining accurate results for these variables, optimization of heat exchanger geometry is performed. The design variable (DV) considered is the inclination angle of louver fins of domain, as used by (Stephan, 2002; Ameel *at al.*,2012).

To execute the optimization study, the commercial code DesignExplorer® from Ansys® is used, selecting the the MOGA procedure; This is an algorithm of evolutionary type, that uses natural selection to generate and choose geometry more efficiently, according to the established objective. There are seven DVs employed which are the fins angles, shown in figure 6.

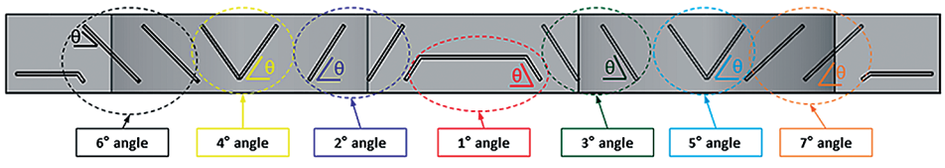

Figure 6
Design variables used for optimization.

To generate the first generation of individuals, the design of experiments of type Optimal Space Filling was used, creating 83 different geometries. The subsequent generations are created selecting the best individuals of previous populations, chosen by maximization of the objective function described below in equation 27.

This expression allows recognizing the global alterations that occurs within the domain, avoiding the use of locally defined factors. The temperature difference in the numerator is used because its augmentation means that more energy was transferred to the cold chain. For the denominator, the pressure differential is used because there is an interest in reducing the pressure losses. So the G expression formed by these two quantities will be maximized by the optimizer algorithm.

$$G = \frac{\Delta T}{\Delta p} \tag{27}$$

3. Results of analysis

Through the expressions 3 to 23 and the Reynolds number obtained in simulation, the Colburn and Fanning factors are calculated and displayed in Figure 7. The curves of numerical results are exhibited with the values obtained from correlations by (Wang *et al.*,1998).

In Figure 7, the red line represents the experimental data, the black lines represent the numerical values and the green lines represent the experimental error variation of 15 % from the experimental test. The simulation reached good accuracy in relation to physical model by (Wang *et al.*,1998).

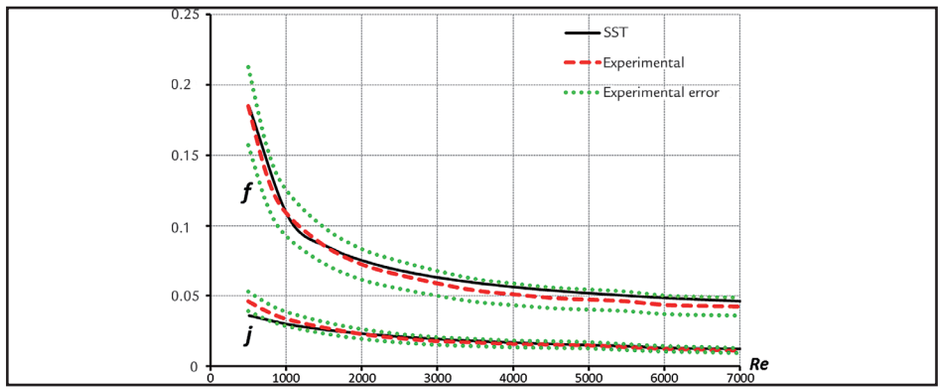

Figure 7
Comparison between numerical and experimental data.

Flow fields and temperature distribution are displayed in Figures 8, 9 and 10, respectively. As can be seen, the points with more intense turbulence are located in the vicinity of V-shaped fins.

Figure 8
Temperature distribution.

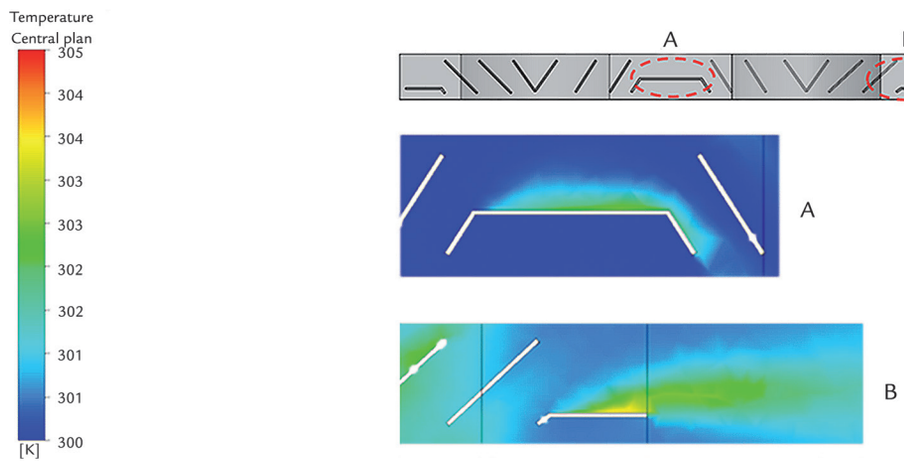

Figure 9
Details of temperature distribution in fins.

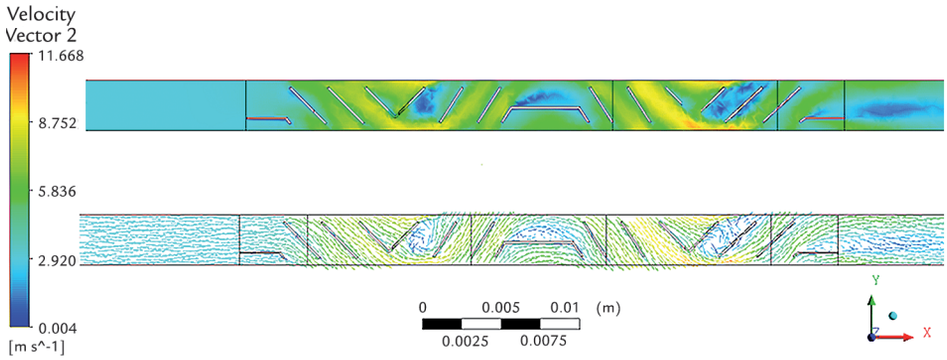

Figure 10
Speed distribution in domain.

To prove that the SST turbulence model is working correctly, Figure 11 shows the distribution of the mixing function values. When the mixing function reaches values below 1, the model *k* - ω is executed along the wall and the model *k* - ω in the rest domain. The blended function contour proves that *k* - ω model is executed near the wall as expected.

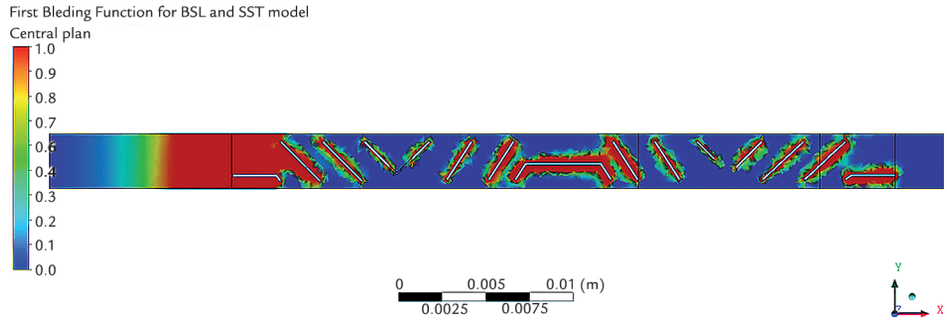

Figure 11
Blended Function.

In Figure 12 is shown the profile of the first generated population using the statistical tool specified in the text. Each broken line represents an individual and each vertical axis represents the value of design variable. The intersection of break line and the vertical axis exhibit a value of this variable for that geometry. The chaotic appearance of this graph demonstrated the variability of individuals in first generation. A good variability of characteristics increases the chances of finding betters performances for heat exchangers.

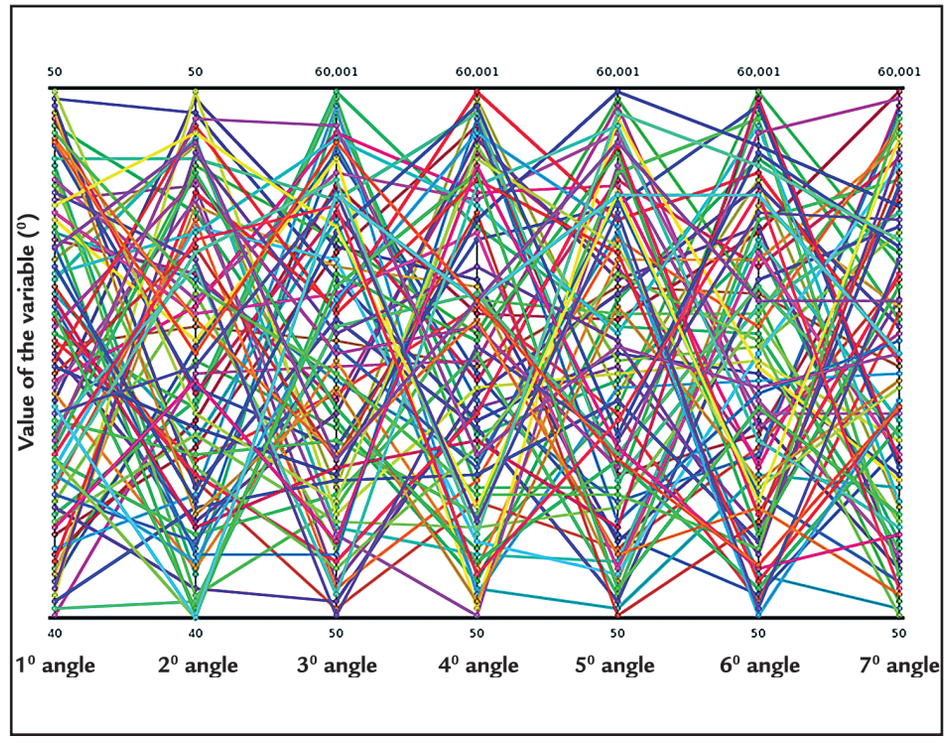

Figure 12
Profile of first generated population.

After the optimization step, the 3 best geometries in all population generated are found, with angles of each louver, exhibited in Table 2. The maximum performance reached was a 25% increase of the objective function.

The analysis of sensibility of design variables in Figure 13, allowed to find the most important fin angles that influence the value of objetive function. For this optization routine, the fifth and seventh are the most influential for optimization results.

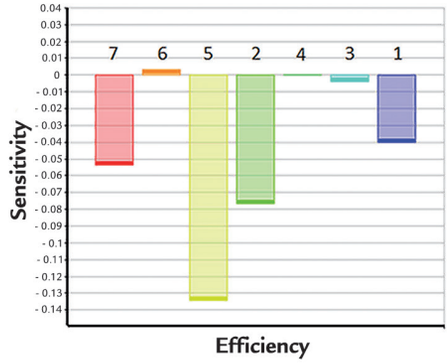

Figure 13
Analysis of DV sensibility.

Angles of Lovers	1	2	3	4	5	6	7	G [°C/Pa]	% increase
Individual A	50.1	50.0	50.0	50.2	59,9	40.9	40.8	0.0046	25.61
Individual B	50.0	50.0	50.0	50.4	58,4	40.6	40.1	0.00454	23.97
Individual C	50.0	50.3	50.2	51.9	59.7	42.8	43.5	0.00439	19.87

Table 2
Values obtained
after optimization with 7 variables.

4. Conclusion

The methodology used in the present paper is efficient for the improvement of the simulated component. The SST turbulence model provided good results when compared to the experimental data and the MOGA evolutionary algorithm provided an increase of approximately 25% for the objective function.

5. Acknowledgements

The authors fully acknowledge the support received from CNPq, FAPEMIG and UFSJ.

6. References

AMEEL, B., DEGROOTE, J., HUISSEUNE, H., JAEGER, P. DE, VIERENDEELS, J., PAEPE, M. DE. Numerical optimization of louvered fin heat exchanger with variable louver angles. ***Journal of Physics, Conference Series,*** v. 395, conferência 1, 2012.

HERCKERT, MATHEUS GUILHERME REIMANN. ***Fluidodinâmica computacional e suas aplicações.*** Uberlândia, MG, Fevereiro, 2004.

JIIN-YUH JANG, CHUN-CHUNG CHEN. Optimization of the louver angle and louver pitch for a louver finned and tube heat exchanger. ***International Journal of Physical Sciences***, v. 8, n.43, p. 2011-2022, 2013.

MALISKA, CLÓVIS R. ***Transferência de calor e Mecânica dos Fluidos Computacional.*** (2.ed.). Rio de Janeiro, RJ: LTC Editora, 2004.

MENTER, F. R. Two-equation eddy-viscosity turbulence models for engineering applications, ***AIAA Journal***, v. 32, n. 8. p. 1598-1605, 1994.

MICHAEL J. LAWSON. ***Practical applications of delta Winglets in Compact Heat Exchangers with louvered fins.*** Instituti Politécnico da Virgínia, 2006. (Master Dissertation).

PERROTIN, THOMAS, CLODIC, DENIS. Thermal-Hydraulic CFD Study in Louvered Fin-and-Flat-Tube Heat Exchangers. ***International Journal of Refrigeration***, v. 27, p. 422-432, p.2004.

STEPHAN, RYAN A. Heat transfer measurements and optimization studies relevant to Louvered Fin Compact Heat Exchangers. Virginia, Blacksburg, 2002. (Master Dissertation in Mecanic Engeneer).

WANG, C. C., LEE, C. J., CHANG, C. T., LIN, S. P. Heat tansfer and friction correlation for Compact Louvered Fin and Tube Heat Exchanger. ***International Journal of Heat and Mass Transfer,*** v. 42, p.1945-1956, 1998.

WEBER, GUSTAVO CARDOSO. Análise experimental do desempenho termo-hidráulico de condensadores do tipo tubo-aletado. Universidade Federal de Santa Catarina, Florianópolis, 2007. (Dissertação de Mestrado).

Received: 25 January 2016 - Accepted: 10 May 2016.